Semiconductors Application in Wastewater Treatment

Subjects: Engineering, Chemical

Contributor: Eryk Fernandes , João Gomes , Rui C. Martins

Photocatalysis has been vastly applied for the removal of contaminants of emerging concern (CECs) and other micropollutants, with the aim of future water reclamation. As a process based upon photon irradiation, materials that may be activated through natural light sources are highly pursued, to facilitate their application and reduce costs. TiO_2 is a reference material, and it has been greatly optimized. However, in its typical configuration, it is known to be mainly active under ultraviolet radiation. Thus, multiple alternative visible light driven (VLD) materials have been intensively studied recently. WO_3 and g-C_3N_4 are currently attractive VLD catalysts, with WO_3 possessing similarities with TiO_2 as a metal oxide, allowing correlations between the knowledge regarding the reference catalyst, and g-C_3N_4 having an interesting and distinct non-metallic polymeric structure with the benefit of easy production.

contaminants of emerging concern | catalysts doping | composite materials | visible photocatalysis | ozonation

1. Introduction

The wastewater treatment plants (WWTPs) are currently responsible for the provision of proper sanitary living conditions for more than 5.2 billion people, but as industries evolve, a large number of different products and chemicals are consumed by the population, eventually making their way into these facilities, which are not designed to treat them [1][2]. There is a great number of these pollutants, but a certain group is particularly important, the contaminants of emerging concern (CECs), which are a variety of chemicals, such as pesticides, pharmaceutical and personal care products (PPCPs), hormones, and stabilizers [3]. Due to their ineffectiveness, WWTPs become a major source of CECs, which may accumulate in the environment and have already been detected, at ng L^{-1} and µg L^{-1} ranges, in surface and groundwater, as well as in remote places, such as high-altitude rivers and the Antarctic Peninsula [4][5][6][7].

Different treatments and techniques have been researched by the scientific community to solve the problem associated with CECs, but a feasible and broad-range solution is yet to be found [8]. Advanced oxidation processes (AOPs) are presented as suitable alternatives for the degradation of a wide range of pollutants, based upon the formation of reactive oxidative species (ROS), most importantly hydroxyl radicals (·OH). AOPs include an array of treatments, vastly explored towards CECs abatements, such as ultraviolet-, ozone-, photocatalysis-, Fenton-, and sulfate-based processes [9][10][11][12] (**Figure 1**). Ozone-based water disinfection treatments are well-established,

but also currently one of the most applied AOP for micropollutants removal, being already implemented as tertiary wastewater treatment in some countries [13].

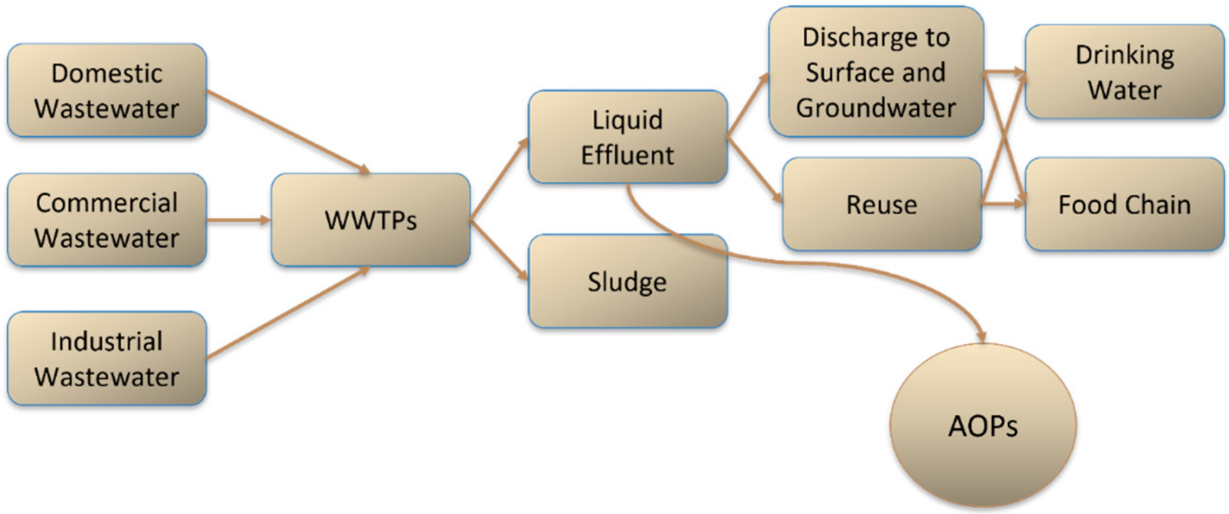

Figure 1. Water treatment scheme and routes of contaminants introduction in the environment.

Ozone is a very strong oxidant, with a redox potential of 2.08 eV, capable of directly reacting with microorganisms and different organic compounds, but it may also be responsible for indirect reactions, producing hydroxyl radicals, which then can interact with the microcontaminants [14]. Nevertheless, this process faces some disadvantages, namely the low solubility of ozone in water, the high energy requirement for its production, low mineralization, and the formation of byproducts potentially more toxic than the parent compounds [15][16]. To enhance the single ozone process, a very common strategy is to integrate or couple it with other AOPs, for instance, O_3/UV, O_3/H_2O_2, O_3/Cl, and O_3/Photocatalysis [9][17][18]. Photocatalytic ozonation is then a promising combined technique, boosting the treatment efficacy and suppressing the individual processes' disadvantages. Photocatalysis is based upon the activation of a catalyst through photon absorption, which then promotes multiple radical's production reactions that attack a large range of contaminants. The contaminants may also be eliminated directly by the catalyst through adsorption [12]. The photocatalysis, when in combination with ozone, can promote a higher decomposition of the gas in water, diminishing ozone demand and increasing the production of ROS. Besides, ozone may also enhance photocatalysis by acting as an electron receiver, reducing electron-hole recombination, which is one of the major disadvantages of this process [19].

Photocatalytic systems are very adaptable and, currently, there is a great variety of catalysts available to be used, the most common being TiO_2. Notwithstanding, TiO_2 presents some disadvantages that challenge its large-scale application, but as these materials are easily tunable, recent studies present multiple adaptations to enhance photocatalysts' performances, such as doping using metal and non-metal elements, immobilization onto other materials, as well as the coupling of different catalysts and materials with distinct natures. Another route is the exploration of alternative catalysts, other than TiO_2, that present superior performances over visible/solar radiation, lowering the process overall cost, which nowadays corresponds to a high-interest field of exploration [20].

Regarding other catalysts, visible-light-driven (VLD) materials became the aim of an increasing number of studies, presenting a better and easier alternative regarding their activation. g-C_3N_4 is a currently very significant catalyst, possessing a metal-free polymeric structure, with simple and very adaptable synthesis methods. Another example, WO_3, also possesses lower bandgap energy and broader absorption of solar radiation while sharing the metal oxide characteristic of TiO_2, which allows an easier correlation between possible known mechanisms and adaptations that can be made. These alternative materials, although with interesting light absorption properties, still face some drawbacks, some also found in TiO_2, such as high electron-hole recombination, low specific surface areas, and improper energy band positions, which hinder the potential of the redox reactions responsible for contaminants elimination.

2. General Features of Catalysts for Photo-based Treatment Processes

Titanium dioxide is certainly the most applied catalyst for photocatalytic water treatment and possesses different crystalline phases, anatase, rutile, and brookite, with anatase having a higher general photocatalytic activity [21].

The benchmarked P25 catalyst was applied by Gomes et al. [22] for the degradation of a complex solution of insecticides, namely azoxystrobin, buprofezin, imidacloprid, procymidone, simazine, terbutryn, and thiamethoxam. Under solar radiation for 120 min, Degussa P25 TiO_2 completely removed 100 µg L^{-1} of almost all pesticides, excluding thiamethoxam (~90%) and procymidone (~50%). The authors also evaluated the scale-up effect, in a pilot-scale 120 L photoreactor, P25 achieved lower degradation yields, expected due to the larger volume, but still favorable, with removal rates higher than 70% with a photon flux of approximately 8 kJ L^{-1}. Photocatalytic ozonation was also assessed, and the higher production of ROS improved the degradation of the insecticides by more than 80%, while single ozonation had considerably lower removal rates for some contaminants, such as Procymidone (~50%) and Imidacloprid (~50%). However, the high electronic density groups characteristics of the contaminants that promote a fast reaction with molecular ozone still allow a noticeably efficient treatment by the single process.

Even with broad usage, TiO_2 faces compromising disadvantages that challenge its full-scale application. Primarily, its high bandgap energy, ~3.2 eV for anatase and ~3.0 eV for rutile TiO_2, makes its photoactivation possible only under UV radiation, with $\lambda \leq 390$ nm, hampering its activation through sunlight as the UV portion represents only 4–6% [12].

Graphitic carbon nitride (g-C_3N_4) is a metal-free semiconductor catalyst, with high photochemical stability and photoelectric properties, that can be obtained through the thermal polymerization of numerous low-price nitrogen-rich organic precursors. It emerges as a promising visible-light-driven photocatalyst, as it possesses a typical absorption edge at 450–470 nm which corresponds to a bandgap energy of approximately 2.7 eV [23]. The graphitic C_3N_4 is the most stable among the multiple allotropic forms of C_3N_4 (e.g., cubic, beta, alpha), due to its particular 2D structure formed by triazine or heptazine rings.

As mentioned, g-C_3N_4 can be synthesized through the polymerization of different precursors, which will intrinsically affect the properties of the photocatalyst. Nguyen et al. [24] evaluated this parameter using dicyandiamide, melamine, urea, and thiourea as g-C_3N_4 precursors. Their physical and optical properties were considerably distinct, with urea-based g-C_3N_4 having noticeably better values, a specific surface area (S_{BET}) more than three times higher than the others (78.9 m^2 g^{-1}), and lower bandgap energy (2.72 eV). The authors also conducted a chemical oxidation treatment over the catalysts, a method used for the exfoliation of g-C_3N_4, improving their properties, such as the surface area, hydrophilicity, and the addition of reactive functional groups (e.g., hydroxyl). The exfoliation treatment resulted in generally higher S_{BET}, pore density, and a slower recombination rate of the photogenerated electron-hole pairs, indicated by the photoluminescence spectra and electrochemical impedance spectroscopy (EIP).

The g-C_3N_4 exfoliation may also be obtained through other methods, such as ultrasonication in water or alcohol solutions, or thermal treatment [23]. Fernandes et al. [25] compared Degussa P25 TiO_2 with dicyandiamide-based g-C_3N_4, subjected to a posterior thermal treatment, for the removal of methyl-, ethyl-, and propylparaben (0.08 mM), individually and in the mixture. Under visible light, the polymeric catalyst achieved complete elimination of parabens within 20 min, individually, and 30 min when in a mixture, while P25 TiO_2 obtained the same results in 120 min. The g-C_3N_4 also proved capable to maintain its stability and efficiency when tested in real water matrices, tap and river water. The thermal exfoliation may also partially remove amino groups and thus introduce defects in the catalyst structure, which reduce electron and hole recombination [26].

Tungsten trioxide (WO_3) is a transition metal oxide that also appears as a promising photocatalyst to be used in chemical and biological CECs removal. The high photostability, corrosion resistance, low-cost fabrication, and bandgap of 2.5–2.8 eV are some of its benefits for photocatalytic usage [23]. Bulk WO_3 possesses a cubic perovskite structure and may be obtained in multiple crystalline forms, such as cubic, hexagonal, and monoclinic, the last being more stable at room conditions, formed between 17 °C and 330 °C.

Different forms of WO_3 catalysts, synthesized through sol-gel and hydrothermal methods, have also been applied for photocatalytic ozonation by Mena et al. [27] for N,N-diethyl-meta-toluamide (DEET) abatement under visible light. Sol-gel monoclinic WO_3 calcinated at higher temperatures (600–700 °C) presented faster removals, eliminating DEET in 10 min. In comparison, over 2 h, the photocatalytic oxidation of DEET achieved only a 22% removal. The presence of ozone in the reaction medium can significantly decrease the typical high recombination rate of the photogenerated species.

3. Catalyst Doping

3.1. TiO_2

TiO_2 is the most used semiconductor catalyst for the photocatalytic elimination of contaminants, but still presents some typical characteristics that hinder the process scale-up. Its high bandgap energy typically implies the use of external UV radiation sources, with $\lambda \leq 390$ nm, hampering its activation through sunlight as the UV portion

represents only 4–6% [12]. The high recombination rate of e^-/h^+ and a weak separation of photocarriers also reduces its photocatalytic activity [28]. Among different modifications, catalyst doping thus appears as a practical technique to overcome these disadvantages.

3.1.1. Transition Metals Doping

Both metal and non-metal elements may be incorporated in the catalyst structure and are capable of altering light absorption capacity and, more importantly, visible light, preventing the recombination of electron-hole [29]. Regarding metal doping, transition metals are more commonly applied, due to their partially filled *d* states, which promote the creation of intra-bandgap energy states and the absorption shift [30].

In reference to the catalyst synthesis, the sol-gel method is one of the main alternatives and allows better control of the product characteristics, such as porosity, structure, composition, and homogeneity, which is especially important in the incorporation of dopants. Moreover, a calcination step post-synthesis is usually applied as a simple technique to transform an amorphous structure into a crystalline (Anatase, Rutile, and Brookite). Karuppasamy et al. [31] attested that, during the investigation of the doping effect of different transition metals (Zn, Cu, and Zr) on TiO_2, the presence of doping elements may also alter the crystalline phase formation, reducing the temperature at the calcination stage needed to achieve the different structures, which was confirmed by other studies [32][33]. Regarding the different elements used and their photocatalytic activity, Zn-TiO_2 presented the best performance in methylene blue elimination under visible light. The interactions between Zn correspondent electronic states with the TiO_2 conduction band may provoke a red shift in the bandgap, improving the material light absorption between 400 nm and 700 nm.

3.1.2. Noble and Rare-Earth Metals Doping

Noble metals (e.g., Au, Ag, Pd, Pt) represent a high-interest group of transition metals currently being vastly explored for TiO_2 doping due to their light-gathering capability and their role as electron trappers. These metals present, in general, a larger ionic radius compared to Ti^{4+}, which difficult their penetration into the catalyst lattice, being deposited mostly on the surface. Saber et al. [34] detected multiple peaks corresponding to the presence of an Au crystalline phase in Au-TiO_2, prepared by solvothermal method, that can be indicative of surface modifications. Additionally, visible light absorption was considerably increased, again attributed to surface plasmon resonance.

Noble metal doping is known to produce a surface plasmon resonance effect, which induces a higher photoactivity of the catalyst under visible irradiation. This effect can be identified through diffuse reflectance spectroscopy (UV-Vis DRS), with a broader shoulder-like peak attributed to the heteroatom addition and the resulting oscillation of the conduction band electrons on its surface during photoirradiation [35]. Moreover, Ellouzi et al. [35] identified such a phenomenon, which resulted in considerable faster degradation of RhB, with an observed rate constant of 0.1827 min^{-1} using a Ag-TiO_2 catalyst, while non-doped TiO_2 led to an apparent constant rate of 0.1034 min^{-1}. The lack of general and more specific legislation and regulation challenges the classification of CECs, but different synthetic

dyes are also considered by many researchers as examples of CECs, due to their potential toxicity, with some studies already appointing their carcinogenic and mutagenic characteristics and ubiquitous behavior [36].

3.1.3. Non-Metals Doping

Non-metal elements (e.g., N, S, B, C) are vastly explored for TiO_2 doping, with facile production methods, and capable of enhancing the catalyst stability and photoactivity, forming new energy levels with the consequent bandgap shortening, and inducing the formation of oxygen vacancies [30]. Contrarily to metals, in non-metal doping, it is expected that the introduced elements will have an influence over the valence band through interactions with O 2p states, even though cationic interactions may also take place [28].

Nitrogen doping is one of the most explored techniques, due to its promising red shift of the absorption edge and a similar ionic radius to oxygen, facilitating its substitution, although it may be inserted in the catalyst structure in different forms [37]. Because of the broad exploration, different preparation methods have been applied, such as pulsed laser deposition [38], thermal annealing [39], hydrothermal [40][41], solvothermal [42], and sol-gel [43][44][45].

The sol-gel method is the most widely applied, due to its facile, flexible, and controllable operation, allowing different modifications of the basic processes to achieve the desired characteristics [46]. Using such a method, Assayehegn et al. [47] synthesized multiple N-TiO_2 catalysts applying different ratios of guanidium chloride (GUA), an environmentally friendly N precursor, to Ti, and indicated that the incorporation of N precursor showed a direct effect over the crystalline phase of N-TiO_2 formation post calcination. This can be caused by the perturbance of N^{3-} ions on the lattice orientation and density of charges, due to its higher negative charges and ionic radius compared to O^{2-}. Moreover, the found optimum mixed crystalline phase, 42% anatase and 58% rutile, is pointed out to have a beneficial synergic effect with nitrogen doping, which was also concluded by other research groups [32][44]. When applied for MB degradation under visible light, the best N-TiO_2 had an apparent reaction rate constant of 0.0325 min^{-1}, which is almost 17 times higher than the undoped catalyst, and represented 97% of MB removal within 100 min.

3.1.4. Co-Doping

The application of two or more dopants can be highly beneficial, as it can enhance the catalyst performance through multiple mechanisms. Multiple combinations of elements are possible and have been explored, even with different classifications, such as metal and non-metal co-doping. The co-doped Fe-Pr-TiO_2 catalyst, studied by Mancuso et al. [48], presented an improved performance regarding AO dye removal compared to the single and undoped catalyst, with 87% removal of the AO and 80% TOC removal in 60 min under visible light. In the studied case, the co-doping was accounted to considerably decrease the E_{bg} (2.7 eV) and enhance the formation of oxygen vacancies, confirmed in photoluminescence spectra, acting as electron trappers, and reducing the e^-/h^+ recombination. The authors also investigated in another study the co-doping of Fe and N, and again it showed a superior performance as it can benefit from both the substitution of Ti^{4+} by Fe^{3+}, acting as electron acceptors and inhibiting e^-/h^+ recombination, and the nitrogen replacement of oxygen sites, producing Ti^{3+} and oxygen vacancies [49].

3.2. WO_3

The WO_3 photocatalysts appear as an interesting alternative to typical TiO_2, with good visible-light activity, but also chemical and electronic properties [50]. However, some drawbacks are still found, principally the high electron-hole recombination rate and a more positive position of the CB, which compromises the superoxide production [46]. The introduction of heteroatoms to the WO_3 structure has not been widely explored compared with other catalysts, but some studies have been conducted showing that this adaptation may be responsible for promoting the enhancement of the catalyst performance and its typical disadvantages.

3.2.1. Transition Metals Doping

WO_3 doping can considerably interfere with basic catalyst characteristics, such as crystallinity, morphology, and optical properties, which will then produce variations in their photocatalytic activity. Cu-WO_3 was found to have a lower E_{bg} (2.78 to 2.60 eV) and higher crystallinity compared to the studied undoped catalyst by Quyen et al. [51]. Besides, changes in its surface properties were also detected, with the incorporation of Cu being mainly at this level, promoting the formation of a more porous structure, meaning a higher surface area and number of active sites capable of enhancing contaminants' interaction and degradation. The presence of the heteroatom also promoted a higher presence of the W^{5+} state, which may imply the equivalent formation of oxygen vacancies due to electronic rebalance, which may increase the catalyst electroconductivity and pollutants adsorption.

3.2.2. Noble and Rare-Earth Metals Doping

The use of different precursors during the photocatalyst and doping synthesis can alter the mechanisms and the configuration of the formed product. Palharim et al. [52] studied the alteration caused by the addition of HCl or HNO_3 during Ag-WO_3 synthesis, using $AgNO_3$ as the dopant precursor. It was found that HNO_3 promoted the incorporation of the dopant metallic silver, while HCl reacted with $AgNO_3$ to form AgCl, being detected in the catalyst structure. This promoted differences in the catalyst, as an increase in Ag concentration led to lower E_{bg} in HNO_3/Ag-WO_3 due to the particle agglomeration, and the opposite occurred for HCl/Ag-WO_3. Regardless of the acid used, Ag-WO_3 had better removal rates of acetaminophen under visible light than the undoped catalyst, because of the combination of factors such as the localized surface plasmon resonance, characteristic of noble metal doping, the insertion of new energy level within the catalyst bandgap and the reduction of E_{bg}. Moreover, HCl doped presented a better performance, possibly due to the interaction between Ag-WO_3 and the AgCl clusters formed, and the contribution towards decreasing the WO_3 conduction band to more negative values, allowing oxygen reduction.

3.2.3. Non-Metals Doping

The combination of the non-metal elements and WO_3 can also promote variations of the CB and VB of the catalyst, hinder the recombination factor of photoinduced charges, and increase photocatalytic activity under visible light. The S-WO_3 nanowires catalyst was investigated by Han et al. [53] using thiourea as the sulfur precursor. The non-metal element was able to substitute W^{6+} in the form of S^{6+} in the WO_3 lattice, as opposed to the anionic replacement of O^{2-}, due to the higher energy form of W-S bonds than W-O. The doping method also accounted for

the formation of surface hydroxyl groups because of oxygen adsorption, which may act as electron trapping centers. Sulfur also was responsible for creating intermediate energy levels above the VB of WO_3, enhancing the catalyst's photoresponse.

3.2.4. Co-Doping

As dopants may have different mechanisms, their combination can severely upgrade the photocatalytic activity through the synergic combined effect, being able to attain higher removal rates, even at complex effluents. Tijani et al. [54] proposed a green synthesis of I-P-WO_3, by applying a plant extract in bulk catalyst production. The I^- and P^{3+} atoms acted as structure-directing agents, affecting the morphology of the rod-like catalyst, with P conducing to more elongated shapes and I with shorter and more uniform. Alterations of lattice parameters indicated distortions of the catalyst structure, which may be a result of the partial substitution of W^{6+} and O^{2-}, by respectively P^{3+}, which has a smaller ionic radius than W, and I^- that has a higher ionic radius compared to O. This substitution is pointed out to have detrimental effects as it may occur the collapsing of the WO_3 structure.

3.3. g-C_3N_4

Even with a typically lower E_{bg} compared to TiO_2, g-C_3N_4 still exhibits a fast recombination rate of the photogenerated e^-/h^+ pairs and a limited light absorption range, which diminishes the visible and solar radiation conversion. Thus, the doping of g-C_3N_4 may contribute to charge separation and concurrently a shift of light absorption. As g-C_3N_4 has gotten much attention recently, investigation of the incorporation of multiple elements over the catalyst structure has been reported.

3.3.1. Metals Doping

The doping using metallic elements is known to promote the formation of oxygen vacancies and considerably improve the catalyst activity. The existence of various unbounded electrons in the hexazine structures of g-C_3N_4 makes it susceptible for metallic elements to be inserted in its lattice [55]. For the removal of paracetamol under visible light, doping using cobalt (II) nitrate was made over a melamine-based g-C_3N_4 through a calcination method [56]. The detected Co^{2+} and Co^{3+} in the catalyst and the O 1s XPS spectra indicated the formation of oxygen vacancies. Moreover, the doping affected the crystallinity of g-C_3N_4 and its morphology, presenting a mixed structure of cobalt oxide closely attached to carbon nitride layers. Optical characterization also showed indirect recombination of charge carriers and smaller charge transfer resistance, which indicates a higher charge transport kinetics and separation. Ultimately, the Co-doped g-C_3N_4 presented a reaction rate almost three times higher than the undoped catalyst, 0.0382 min^{-1}, completely removing 1 mg L^{-1} of paracetamol within 120 min. No leaching of Co ions was detected after the oxidation experiments.

3.3.2. Noble and Rare-Earth Metals Doping

Noble metals, such as Ag and Au, are electron-rich transition metal elements that can capture photogenerated electrons and provide the excess energy of plasmonic states, provoking a shift of the Fermi levels to less positive potentials due to an excess of negative charges, reducing electron-hole recombination and boosting its catalytic

performance. Tri et al. [57] explored Ag-doped g-C_3N_4 for the treatment of tetracycline, an antibiotic, in hospital wastewater under solar irradiation. Besides the faster production and higher separation of the e^-/h^+, Ag significantly altered the optical properties of the catalyst, decreasing its E_{bg} down to 2.19 eV, and possibly increasing the number of active sites and surface area, culminating in an optimum removal of 96.8% of tetracycline under 120 min.

3.3.3. Non-Metals Doping

Non-metal and metalloid elements have a larger record of use in g-C_3N_4 doping and are able to overcome the disadvantageous surface characteristics of the catalyst and improve its electronic and optical properties. Zhang et al. [58] synthesized a mesoporous g-C_3N_4 which presented a high specific surface area, 91.1 m^2 g^{-1}, due to its porous structure, providing a larger number of active sites. However, due to the quantum size effect, the UV-Vis absorption spectrum suffered a blue shift as bandwidth decreased with the concurrent decrease of particle size. It was found that oxygen doping, besides the reduction of the photo-induced carriers' recombination, may compensate for the absorption blue shift and enhance photocatalytic activity under simulated solar irradiation. The oxygen-doped mesoporous catalyst attained incredibly faster quasi-first-order kinetic constants for RhB and MO degradation, 64 and 24 times higher than simple mesoporous g-C_3N_4.

3.3.4. Co-Doping

The use of multiple elements simultaneously for the doping of g-C_3N_4 has already been explored, albeit with fewer studies, and has shown a great boost in the material photoactivity. The most significant feature of g-C_3N_4 co-doping is appointed to be an improvement in electron mobility [59]

3.4. Overall Considerations

The application of catalyst doping is a well-researched subject, noticeably producing positive effects regarding the improvement of photocatalytic activity. However, even with promising results, some considerations must be taken.

The similarities between the structures of WO_3 and TiO_2 as metal oxides allow analogous modification mechanisms to occur, providing great support as TiO_2 is already the subject of a great amount of research and information as it has been intensively optimized.

Rare-earth and noble metals provide excellent alterations, especially on the crystalline and electronic structure, due to the existence of more electron-rich orbitals, as well as their optical properties, e.g., through surface plasmon resonance. However, the sometimes complex and difficult impregnation of such elements, and their typically higher cost, need to be evaluated, although their use in small quantities can already provide significant results.

Other metallic elements can be an easier alternative, with comparatively lower costs regarding materials and impregnation techniques. In the case of g-C_3N_4, the exploration of transition metals doping is more widely explored, possibly due to the more distinct nature between the foreign and existent elements, which can provide more evident effects. These elements may lead to the easier formation of new energy sublevels and shift the light

absorption to higher wavelengths. Such electronic interaction, especially as it occurs mainly with the conduction band of the catalysts, is also a great improvement for the less negative conduction band of WO_3, which difficult its reduction potential. The ozonide radical formation can also be enhanced by the modification of the conduction band, in the case of photocatalytic ozonation, facilitating the capture of electrons by ozone.

4. Composite Catalysts

With the increasing conceptualization of different catalysts, the combination of different materials emerges to present a wide number of possibilities to improve the overall catalytic properties [60]. By mixing materials with different characteristics, their individual disadvantages may be overcome, and a final and more robust photocatalyst can be obtained. These composites are then a combination of materials with distinct natures, such as mixed metal oxides, carbon-semiconductors, polymeric structures, porous materials, and many others.

The mixing of WO_3 and TiO_2 is a clear example of mixed metal oxides, a well-known group of photocatalysts defined by the combination of different semiconductors. The coupling of these photocatalysts aims to improve the photocatalytic activity of the resultant material by mostly increasing the charges separation efficiency and visible-light sensitization for the complete system [61]. Mugunthan et al. [62] proved the higher efficiency of the coupled TiO_2/WO_3 catalyst for diclofenac elimination under visible radiation. The group synthesized the photocatalyst through a hydrothermal method and studied the variation of TiO_2:WO_3 molar ratios. The composites presented higher surface areas and smaller particles compared to bare TiO_2, with the increasing amount of TiO_2 leading to larger S_{BET}, bus also particle sizes, and E_{bg}. Thus, an optimum TiO_2:WO_3 molar ratio (10:1), presented more balanced properties and higher removal of diclofenac (~90%). An excess amount of WO_3 is also appointed to possibly act as recombination centers for the photoinduced charges, reducing the process efficiency.

The surplus addition of one of the applied semiconductors can also promote the agglomeration of photocatalyst particles, which may hinder the absorption of light and CECs photodegradation, as it was suggested by El-Yazeed and Ahmed [63] during the impregnation of WO_3 particles onto TiO_2, which had a detrimental effect over a concentration of 10 wt%. This was also found by Wang et al. [64] for hollow spherical TiO_2/WO_3 composite, with uniform spheres being formed with a 5 wt% incorporation of WO_3, but with the further increase in concentration and particle agglomeration causing changes in the catalyst morphology and leading to flat and unequal forms. However, in the study, the catalyst containing 10 wt% WO_3 had a better performance in methylene blue and metoprolol degradation, due to the photoelectronic and surface area improvements.

The TiO_2-WO_3 heterojunction can greatly improve the photo-mechanisms involved in the photocatalytic process. Considering their bandgap positions, the charge separation can follow two mechanisms: type-II heterojunctions or Z-scheme mechanisms. For the type-II mechanism, the excited electrons from the CB of TiO_2, which has a more negative potential, will migrate to the CB of WO_3. Meanwhile, the opposite occurs in the positive holes, which tend to be transferred to the TiO_2 VB [65]. Nonetheless, the Z-scheme mechanism is appointed to be more favorable due to the larger redox potential, as the e^- of the CB of WO_3 and h^+ of the VB of TiO_2 tend to recombine fast, leading to

the accumulation of e^- on the CB of TiO_2 and h^+ on the VB of WO_3, potentializing its respective reductive and oxidative potential [66].

4.1. TiO_2

Over the years, TiO_2 was vastly employed in the production of different composite catalysts, allowing a better understanding of their overall mechanisms and advantages. The coupling of TiO_2 with other photocatalytic materials appeared as a vast family of mixed catalysts, with combined improved properties. Due to the existence of multiple photocatalysts, numerous combination possibilities are the aim of a rising number of investigations.

Zinc Oxide (ZnO) is, jointly with TiO_2, one of the most investigated semiconductors for contaminants removal, sharing their good photochemical characteristics but with relatively better electrical properties. Nonetheless, their heterostructures have been explored in different forms and systems for pollutant elimination. The increasing addition of ZnO in ZnO/TiO_2 fibers has been shown to also promote changes in the physical properties of the material, creating a rougher surface with a higher specific surface area and faster interaction with contaminants [67]. Changes in the morphology of the material have been also attested. Das et al. [68], indicated the transformation of uniform rod-like structures of ZnO into more of a flower-like form by the addition of TiO_2, with the enhancement of the BET surface until an optimal amount. A lower recombination rate of the electron-hole pairs was also demonstrated, increasing the lifespan of the photoinduced charge carriers.

The combination of TiO_2 with bismuth-based materials is a topic that gained much attention, as this family of compounds presents a series of attractive features, such as their low toxicity, easy functionalization, cost-effectiveness, and ability to absorb in near infra-red regions. Some examples of the most studied Bi-based photocatalysts are bismuth oxide (Bi_2O_3), bismuth vanadate ($BiVO_4$), and bismuth oxyhalide (BiOX), involving combination with halogen elements (X) [69][70][71].

The $BiVO_4$/N-TiO_2 heterostructure synthesized by Cipagauta-Díaz et al. [69] presented increased specific surface areas and absorption of visible light with the increasing $BiVO_4$ content. The catalyst also presented zones of heterogeneity that allow contact between the semiconductors and improve the separation of photogenerated charges and the lifetime of charge carriers. Ultimately, the best composite catalyst resulted in 98% removal of ofloxacin under 90 min. Even with the morphology and light absorption properties improvement, an excessive amount of $BiVO_4$ (>5 wt%) was demonstrated to be prejudicial to the photocatalytic performance, possibly due to the formation of $BiVO_4$ agglomerates in the catalyst surface, which hamper the homogeneous light absorption.

4.2. WO_3

To overcome WO_3 drawbacks and obtain a more robust photocatalytic material, various hybrid structures have been explored. The coupling with other metal oxides and semiconductors is more substantially pursued, possibly as a more facile approach to surpass its high electron-hole recombination rate, and the less negative conduction band and compromised reductive potential, as it can benefit from the electron-hole interaction of the formed heterojunctions.

In recent years, phosphate-based photocatalysts, especially Ag_3PO_4, have been the focus of numerous studies due to their superior quantum efficiency under visible light irradiation, 90% [20]. However, it still faces relatively large particle sizes (0.5–2 µm), instability, and photo-corrosion, hindering a highly efficient photoactivity and its recyclability. Thus, Ag_3PO_4 and WO_3 composites may benefit from their heterostructures and be presented as more robust photocatalysts.

The instability of Ag_3PO_4 can be further increased by adding other components with better electronic properties. Graphene, which can be doped to boost its characteristics, is an excellent electron mediator and has been demonstrated to significantly increase the recyclability of Ag_3PO_4/WO_3 composites, providing higher chemical stability, surface area, and electron mobility by the organic material on the ternary composite [72].

4.3. g-C_3N_4

The characteristics of graphitic carbon nitride that hinder its broader utilization, such as its low specific surface area, obstructed active sites, and visible light utilization, can be strongly surpassed by the construction of composite materials. Its polymeric structure may be linked to other materials, with their own photocatalytic properties or characteristics that can boost the g-C_3N_4 performance.

There is an expanding number of studies regarding the combination of g-C_3N_4 with other polymeric materials. Their typically low-cost production, large surface areas, and presence of different functional groups and electrostatic charges can enhance pollutants interaction. Polyethyleneimine (PEI), for example, is a cationic polymer containing many amino groups that have been used in combination with catalyst and carbon-based materials to enhance the electrochemical properties and overall activity of composites. Yan et al. [73] synthesized in one step a PEI/g-C_3N_4 composite through the thermal copolymerization of urea mixed with PEI, obtaining a tremella-like structure containing -NH_X groups, that may be beneficial for water dispersion and photon absorption, and an increased BET surface area, up to 250%. The best composite catalyst also presented 80% removal of tetracycline with a reaction rate constant of 0.0226 min^{-1}, 3.2 times higher than g-C_3N_4. The efficiency of PEI/g-C_3N_4 has also been attested for disinfection purposes, by Zeng et al. [74], resulting in 6.2 and 4.2 log reductions of *E. coli* and *E. faecalis* in 45 and 60 min, respectively. PEI can increase O_2 reduction and alter the surface charges of the catalyst, promoting the adhesion of bacteria through electrostatic attraction.

5. Conclusions

The application of semiconductors in photocatalytic based for CECs abatement has shown remarkable potential as a water treatment technology. The production of highly oxidative radicals may eliminate a variety of these chemical and biological compounds that represent a danger to human and environmental health. These treatments have been pointed out to be effective even in more complex matrices, which proves their capacity to be applied to real effluents under different conditions. The use of additional oxidants such as ozone can also boost the overall process efficiency, increasing the production of radicals and electron retrieval.

The investigations regarding new visible light active photocatalysts show promising results, but more complete studies still need to be conducted to collect more information. The applications of doping and composite materials open a great variety of possibilities for materials with more robust and feasible characteristics to be obtained. Thus, more elaborative comparisons between the new and standard semiconductors and their adaptations need to be performed, to better understand the advantages of further exploration of the already well-founded TiO_2 based materials and the development of alternative materials. The addition of ozone in the photocatalytic process has been proven to enhance the overall efficiency, and more studies of its application with alternative and adapted catalysts will be valuable. Nonetheless, the photocatalytic-based process is a favorable route for the degradation of pathogens and CECs and future large-scale water reclamation technologies.

References

1. McCance, W.; Jones, O.A.H.; Cendón, D.I.; Edwards, M.; Surapaneni, A.; Chadalavada, S.; Wang, S.; Currell, M. Combining Environmental Isotopes with Contaminants of Emerging Concern (CECs) to Characterise Wastewater Derived Impacts on Groundwater Quality. Water Res. 2020, 182, 1–15.
2. Rizzo, L.; Malato, S.; Antakyali, D.; Beretsou, V.G.; Đolić, M.B.; Gernjak, W.; Heath, E.; Ivancev-Tumbas, I.; Karaolia, P.; Lado Ribeiro, A.R.; et al. Consolidated vs New Advanced Treatment Methods for the Removal of Contaminants of Emerging Concern from Urban Wastewater. Sci. Total Environ. 2019, 655, 986–1008.
3. Valbonesi, P.; Pro, M.; Vasumini, I.; Fabbri, E. Contaminants of Emerging Concern in Drinking Water: Quality Assessment by Combining Chemical and Biological Analysis. Sci. Total Environ. 2021, 758, 143624.
4. Olalla, A.; Moreno, L.; Valcárcel, Y. Prioritisation of Emerging Contaminants in the Northern Antarctic Peninsula Based on Their Environmental Risk. Sci. Total Environ. 2020, 742, 140417.
5. Lencioni, V.; Bellamoli, F.; Paoli, F. Multi-Level Effects of Emerging Contaminants on Macroinvertebrates in Alpine Streams: From DNA to the Ecosystem. Ecol. Indic. 2020, 117, 106660.
6. Llamas-dios, M.I.; Vadillo, I.; Jiménez-gavilán, P.; Candela, L.; Corada-fernández, C. Assessment of a Wide Array of Contaminants of Emerging Concern in a Mediterranean Water Basin (Guadalhorce River, Spain): Motivations for an Improvement of Water Management and Pollutants Surveillance. Sci. Total Environ. 2021, 788, 147822.
7. Tian, Z.; Wark, D.A.; Bogue, K.; James, C.A. Suspect and Non-Target Screening of Contaminants of Emerging Concern in Streams in Agricultural Watersheds. Sci. Total Environ. 2021, 795, 148826.

8. Shah, A.I.; Din Dar, M.U.; Bhat, R.A.; Singh, J.P.; Singh, K.; Bhat, S.A. Prospectives and Challenges of Wastewater Treatment Technologies to Combat Contaminants of Emerging Concerns. Ecol. Eng. 2020, 152, 105882.
9. Liu, Z.; Demeestere, K.; Hulle, S. Van Comparison and Performance Assessment of Ozone-Based AOPs in View of Trace Organic Contaminants Abatement in Water and Wastewater: A Review. J. Environ. Chem. Eng. 2021, 9, 105599.
10. Giwa, A.; Yusuf, A.; Balogun, H.A.; Sambudi, N.S.; Bilad, M.R.; Adeyemi, I.; Chakraborty, S.; Curcio, S. Recent Advances in Advanced Oxidation Processes for Removal of Contaminants from Water: A Comprehensive Review. Process Saf. Environ. Prot. 2021, 146, 220–256.
11. Sgroi, M.; Snyder, S.; Roccaro, P. Comparison of AOPs at Pilot Scale: Energy Costs for Micro-Pollutants Oxidation, Disinfection by-Products Formation and Pathogens Inactivation. Chemosphere 2021, 273, 128527.
12. Khan, J.A.; Sayed, M.; Khan, S.; Shah, N.S.; Dionysiou, D.D.; Boczkaj, G. Advanced Oxidation Processes for the Treatment of Contaminants of Emerging Concern. In Contaminants of Emerging Concern in Water and Wastewater: Advanced Treatment Processes; Elsevier Inc.: Cambridge, MA, USA, 2019; pp. 299–365. ISBN 9780128135617.
13. Itzel, F.; Gehrmann, L.; Bielak, H.; Ebersbach, P.; Boergers, A.; Herbst, H.; Maus, C.; Simon, A.; Dopp, E.; Hammers-Wirtz, M.; et al. Investigation of Full-Scale Ozonation at a Municipal Wastewater Treatment Plant Using a Toxicity-Based Evaluation Concept. J. Toxicol. Environ. Health—Part A Curr. Issues 2017, 80, 1242–1258.
14. Irani, R.; Khoshfetrat, A.B.; Forouzesh, M. Real Municipal Wastewater Treatment Using Simultaneous Pre and Post-Ozonation Combined Biological Attached Growth Reactor: Energy Consumption Assessment. J. Environ. Chem. Eng. 2021, 9, 104595.
15. Gulde, R.; Rutsch, M.; Clerc, B.; Schollée, J.E.; von Gunten, U.; McArdell, C.S. Formation of Transformation Products during Ozonation of Secondary Wastewater Effluent and Their Fate in Post-Treatment: From Laboratory- to Full-Scale. Water Res. 2021, 200, 117200.
16. Fernandes, E.; Contreras, S.; Medina, F.; Martins, R.C.; Gomes, J. N-Doped Titanium Dioxide for Mixture of Parabens Degradation Based on Ozone Action and Toxicity Evaluation: Precursor of Nitrogen and Titanium Effect. Process Saf. Environ. Prot. 2020, 138, 80–89.
17. Sgroi, M.; Anumol, T.; Vagliasindi, F.G.A.; Snyder, S.A.; Roccaro, P. Comparison of the New Cl2/O3/UV Process with Different Ozone- and UV-Based AOPs for Wastewater Treatment at Pilot Scale: Removal of Pharmaceuticals and Changes in Fluorescing Organic Matter. Sci. Total Environ. 2021, 765, 142720.
18. Cai, Q.Q.; Jothinathan, L.; Deng, S.H.; Ong, S.L.; Ng, H.Y.; Hu, J.Y. Fenton- and Ozone-Based AOP Processes for Industrial Effluent Treatment; Elsevier: Amsterdam, The Netherlands, 2021;

ISBN 9780128210116.

19. Fernandes, E.; Martins, R.C.; Gomes, J. Photocatalytic Ozonation of Parabens Mixture Using 10% N-TiO2 and the Effect of Water Matrix. Sci. Total Environ. 2020, 718, 137321.
20. Dong, P.; Xi, X.; Hou, G. Typical Non–TiO2-Based Visible-Light Photocatalysts. In Semiconductor Photocatalysis—Materials, Mechanisms and Applications; BoD–Books on Demand: Norderstedt, Germany, 2016; pp. 209–229.
21. Barakat, M.A.; Kumar, R. Photocatalytic Activity Enhancement of Titanium Dioxide Nanoparticles; Springer: Cham, Switzerland, 2016; ISBN 9783319242699.
22. Gomes, J.; Roccamante, M.; Contreras, S.; Medina, F.; Oller, I.; Martins, R.C. Scale-up Impact over Solar Photocatalytic Ozonation with Benchmark-P25 and N-TiO2 for Insecticides Abatement in Water. J. Environ. Chem. Eng. 2021, 9, 104915.
23. García-López, E.I.; Palmisano, L. (Eds.) Material Science in Photocatalysis; Elsevier: Amsterdam, The Netherlands, 2021; ISBN 9781119130536.
24. Nguyen, T.K.A.; Pham, T.T.; Nguyen-Phu, H.; Shin, E.W. The Effect of Graphitic Carbon Nitride Precursors on the Photocatalytic Dye Degradation of Water-Dispersible Graphitic Carbon Nitride Photocatalysts. Appl. Surf. Sci. 2021, 537, 148027.
25. Fernandes, R.A.; Sampaio, M.J.; Dražić, G.; Faria, J.L.; Silva, C.G. Efficient Removal of Parabens from Real Water Matrices by a Metal-Free Carbon Nitride Photocatalyst. Sci. Total Environ. 2020, 716, 135346.
26. Orge, C.A.; Sampaio, M.J.; Faria, J.L.; Pereira, M.F.R.; Silva, C.G. Efficiency and Stability of Metal-Free Carbon Nitride in the Photocatalytic Ozonation of Oxamic Acid under Visible Light. J. Environ. Chem. Eng. 2020, 8, 104172.
27. Mena, E.; Rey, A.; Contreras, S.; Beltrán, F.J. Visible Light Photocatalytic Ozonation of DEET in the Presence of Different Forms of WO3. Catal. Today 2015, 252, 100–106.
28. Huang, F.; Yan, A.; Zhao, H. Influences of Doping on Photocatalytic Properties of TiO2 Photocatalyst. In Semiconductor Photocatalysis: Materials, Mechanisms and Applications; InTech: Osaka, Japan, 2016; pp. 31–80.
29. Basavarajappa, P.S.; Patil, S.B.; Ganganagappa, N.; Reddy, K.R.; Raghu, A.V.; Reddy, C.V. Recent Progress in Metal-Doped TiO2, Non-Metal Doped/Codoped TiO2 and TiO2 Nanostructured Hybrids for Enhanced Photocatalysis. Int. J. Hydrogen Energy 2020, 45, 7764–7778.
30. Varma, K.S.; Tayade, R.J.; Shah, K.J.; Joshi, P.A.; Shukla, A.D.; Gandhi, V.G. Photocatalytic Degradation of Pharmaceutical and Pesticide Compounds (PPCs) Using Doped TiO2 Nanomaterials: A Review. Water-Energy Nexus 2020, 3, 46–61.

31. Karuppasamy, P.; Ramzan Nilofar Nisha, N.; Pugazhendhi, A.; Kandasamy, S.; Pitchaimuthu, S. An Investigation of Transition Metal Doped TiO2 photocatalysts for the Enhanced Photocatalytic Decoloration of Methylene Blue Dye under Visible Light Irradiation. J. Environ. Chem. Eng. 2021, 9, 105254.
32. Lee, H.; Jang, H.S.; Kim, N.Y.; Joo, J.B. Cu-Doped TiO2 Hollow Nanostructures for the Enhanced Photocatalysis under Visible Light Conditions. J. Ind. Eng. Chem. 2021, 99, 352–363.
33. Moreira, A.J.; Malafatti, J.O.D.; Giraldi, T.R.; Paris, E.C.; Pereira, E.C.; de Mendonça, V.R.; Mastelaro, V.R.; Freschi, G.P.G. Prozac® Photodegradation Mediated by Mn-Doped TiO2 Nanoparticles: Evaluation of by-Products and Mechanisms Proposal. J. Environ. Chem. Eng. 2020, 8, 104543.
34. Saber, N.B.; Mezni, A.; Alrooqi, A.; Altalhi, T. Fabrication of Efficient 2/RGO Heterojunction Nanocomposite: Boosted Photocatalytic Activity under Ultraviolet and Visible Light Irradiation. J. Mater. Res. Technol. 2021, 12, 2238–2246.
35. Ellouzi, I.; Bouddouch, A.; Bakiz, B.; Benlhachemi, A.; Abou Oualid, H. Glucose-Assisted Ball Milling Preparation of Silver-Doped Biphasic TiO2 for Efficient Photodegradation of Rhodamine B: Effect of Silver-Dopant Loading. Chem. Phys. Lett. 2021, 770, 138456.
36. Ribeiro, A.R.; Umbuzeiro, G. de A. Effects of a Textile Azo Dye on Mortality, Regeneration, and Reproductive Performance of the Planarian, Girardia Tigrina. Environ. Sci. Eur. 2014, 26, 1–8.
37. Gusain, R.; Kumar, N.; Ray, S.S. Factors Influencing the Photocatalytic Activity of Photocatalysts in Wastewater Treatment. In Photocatalysts in Advanced Oxidation Processes for Wastewater Treatment; John Wiley & Sons: Hoboken, NJ, USA, 2020; pp. 229–270.
38. Mirzaei, A.; Eddah, M.; Roualdes, S.; Ma, D.; Chaker, M. Multiple-Homojunction Gradient Nitrogen Doped TiO2 for Photocatalytic Degradation of Sulfamethoxazole, Degradation Mechanism, and Toxicity Assessment. Chem. Eng. J. 2021, 422, 130507.
39. Ramezanisani, S.; Rajabi, M.; Mohseni, F. Influence of Nitrogen Doping on Visible Light Photocatalytic Activity of TiO2 Nanowires with Anatase-Rutile Junction. Chem. Phys. Lett. 2020, 744, 137217.
40. Suwannaruang, T.; Kamonsuangkasem, K.; Kidkhunthod, P.; Chirawatkul, P.; Saiyasombat, C.; Chanlek, N.; Wantala, K. Influence of Nitrogen Content Levels on Structural Properties and Photocatalytic Activities of Nanorice-like N-Doped TiO2 with Various Calcination Temperatures. Mater. Res. Bull. 2018, 105, 265–276.
41. Erdogan, N.; Bouziani, A.; Park, J.; Micusik, M.; Kim, S.Y.; Majkova, E.; Omastova, M.; Ozturk, A. Synthesis and Enhanced Photocatalytic Activity of Nitrogen-Doped Triphasic TiO2 Nanoparticles. J. Photochem. Photobiol. A Chem. 2019, 377, 92–100.

42. Toe, E.D.; Kurniawan, W.; Mariquit, E.G.; Hinode, H. Synthesis of N-Doped Mesoporous TiO2 by Facile One-Step Solvothermal Process for Visible Light Photocatalytic Degradation of Organic Pollutant. J. Environ. Chem. Eng. 2018, 6, 5125–5134.
43. Yadav, V.; Saini, V.K.; Sharma, H. How Different Dopants Leads to Difference in Photocatalytic Activity in Doped TiO2? Ceram. Int. 2020, 46, 27308–27317.
44. Bakre, P.V.; Tilve, S.G.; Shirsat, R.N. Influence of N Sources on the Photocatalytic Activity of N-Doped TiO2. Arab. J. Chem. 2020, 13, 7637–7651.
45. Zhao, W.; Liu, S.; Zhang, S.; Wang, R.; Wang, K. Preparation and Visible-Light Photocatalytic Activity of N-Doped TiO2 by Plasma-Assisted Sol-Gel Method. Catal. Today 2019, 337, 37–43.
46. Coronado, J.M.; Fresno, F.; Hernández-Alonso, M.D.; Portela, R. Design of Advanced Photocatalytic Materials for Energy and Environmental Applications; Springer: London, UK, 2013; Volume 71, ISBN 9781447150602.
47. Assayehegn, E.; Solaiappan, A.; Chebude, Y.; Alemayehu, E. Fabrication of Tunable Anatase/Rutile Heterojunction N/TiO2 Nanophotocatalyst for Enhanced Visible Light Degradation Activity. Appl. Surf. Sci. 2020, 515, 145966.
48. Mancuso, A.; Sacco, O.; Vaiano, V.; Sannino, D.; Pragliola, S.; Venditto, V.; Morante, N. Visible Light Active Fe-Pr Co-Doped TiO2 for Water Pollutants Degradation. Catal. Today 2021.
49. Mancuso, A.; Sacco, O.; Sannino, D.; Pragliola, S.; Vaiano, V. Enhanced Visible-Light-Driven Photodegradation of Acid Orange 7 Azo Dye in Aqueous Solution Using Fe-N Co-Doped TiO2. Arab. J. Chem. 2020, 13, 8347–8360.
50. Razali, N.A.M.; Salleh, W.N.W.; Aziz, F.; Jye, L.W.; Yusof, N.; Ismail, A.F. Review on Tungsten Trioxide as a Photocatalysts for Degradation of Recalcitrant Pollutants. J. Clean. Prod. 2021, 309, 127438.
51. Quyen, V.T.; Kim, J.T.; Park, P.M.; Huong, P.T.; Viet, N.M.; Thang, P.Q. Enhanced the Visible Light Photocatalytic Decomposition of Antibiotic Pollutant in Wastewater by Using Cu Doped WO3. J. Environ. Chem. Eng. 2021, 9, 104737.
52. Palharim, P.H.; Fusari, B.L.D.d.R.; Ramos, B.; Otubo, L.; Teixeira, A.C.S.C. Effect of HCl and HNO3 on the Synthesis of Pure and Silver-Based WO3 for Improved Photocatalytic Activity under Sunlight. J. Photochem. Photobiol. A Chem. 2022, 422, 113550.
53. Han, F.; Li, H.; Fu, L.; Yang, J.; Liu, Z. Synthesis of S-Doped WO3 Nanowires with Enhanced Photocatalytic Performance towards Dye Degradation. Chem. Phys. Lett. 2016, 651, 183–187.
54. Tijani, J.O.; Ugochukwu, O.; Fadipe, L.A.; Bankole, M.T.; Abdulkareem, A.S.; Roos, W.D. Photocatalytic Degradation of Local Dyeing Wastewater by Iodine-Phosphorus Co-Doped

Tungsten Trioxide Nanocomposites under Natural Sunlight Irradiation. J. Environ. Manag. 2019, 236, 519–533.

55. Ma, T.; Shen, Q.; Xue, B.Z.J.; Guan, R.; Liu, X.; Jia, H.; Xu, B. Facile Synthesis of Fe-Doped g-C3N4 for Enhanced Visible-Light Photocatalytic Activity. Inorg. Chem. Commun. 2019, 107, 107451.
56. Pham, T.H.; Park, J.W.; Kim, T.Y. Enhanced Photodegradation of Paracetamol from Water by Cobalt Doped Graphitic Carbon Nitride. Sol. Energy 2021, 215, 151–156.
57. Tri, N.L.M.; Kim, J.; Giang, B.L.; Tahtamouni, T.M.A.; Huong, P.T.; Lee, C.; Viet, N.M.; Trung, D.Q. Ag-Doped Graphitic Carbon Nitride Photocatalyst with Remarkably Enhanced Photocatalytic Activity towards Antibiotic in Hospital Wastewater under Solar Light. J. Ind. Eng. Chem. 2019, 80, 597–605.
58. Zhang, B.; Li, X.; Zhao, Y.; Song, H.; Wang, H. Facile Synthesis of Oxygen Doped Mesoporous Graphitic Carbon Nitride with High Photocatalytic Degradation Efficiency under Simulated Solar Irradiation. Colloids Surfaces A Physicochem. Eng. Asp. 2019, 580, 123736.
59. Ganganboina, A.B.; Nguyen, M.D.; Nguyen, T.H.L.; Kuncoro, E.P.; Doong, R.-A. Boron and Phosphorus Co-Doped One-Dimensional Graphitic Carbon Nitride for Enhanced Visible-Light-Driven Photodegradation of Diclofenac. Chem. Eng. J. 2021, 425, 131520.
60. Pandit, B.B.; Sonawane, S.; Aniruddha, V.P. (Eds.) Handbook of Nanomaterials for Wastewater Treatment: Fundamental and Scale Up Issues, 1st ed.; Elsevier: Amsterdam, The Netherlands, 2021; ISBN 9789896540821.
61. Khan, M.M.; Pradhan, D.; Sohn, Y. (Eds.) Nanocomposites for Visible Light-Induced Photocatalysis; Springer: Berlin/Heidelberg, Germany, 2017; ISBN 9783319624457.
62. Mugunthan, E.; Saidutta, M.B.; Jagadeeshbabu, P.E. Visible Light Assisted Photocatalytic Degradation of Diclofenac Using TiO2-WO3 Mixed Oxide Catalysts. Environ. Nanotechnol. Monit. Manag. 2018, 10, 322–330.
63. El-Yazeed, W.S.A.; Ahmed, A.I. Photocatalytic Activity of Mesoporous WO3/TiO2 Nanocomposites for the Photodegradation of Methylene Blue. Inorg. Chem. Commun. 2019, 105, 102–111.
64. Wang, Q.; Zhang, W.; Hu, X.; Xu, L.; Chen, G.; Li, X. Hollow Spherical WO3/TiO2 Heterojunction for Enhancing Photocatalytic Performance in Visible-Light. J. Water Process Eng. 2021, 40, 101943.
65. Su, X.; Liu, C.j.; Liu, Y.; Yang, Y.; Liu, X.; Chen, S. Construction of BiVO4 3 Arrays Heterojunction Photoanodes by Versatile Phase Transformation Strategy. Trans. Nonferrous Met. Soc. China 2021, 31, 533–544.

66. Meng, S.; Sun, W.; Zhang, S.; Zheng, X.; Fu, X.; Chen, S. Insight into the Transfer Mechanism of Photogenerated Carriers for WO3/TiO2 Heterojunction Photocatalysts: Is It the Transfer of Band-Band or Z-Scheme? Why? J. Phys. Chem. C 2018, 122, 26326–26336.
67. Someswararao, M.V.; Dubey, R.S.; Subbarao, P.S.V. Electrospun Composite Nanofibers Prepared by Varying Concentrations of TiO2/ZnO Solutions for Photocatalytic Applications. J. Photochem. Photobiol. 2021, 6, 100016.
68. Das, A.; Kumar, P.M.; Bhagavathiachari, M.; Nair, R.G. Hierarchical ZnO-TiO2 Nanoheterojunction: A Strategy Driven Approach to Boost the Photocatalytic Performance through the Synergy of Improved Surface Area and Interfacial Charge Transport. Appl. Surf. Sci. 2020, 534, 147321.
69. Cipagauta-Díaz, S.; Estrella-González, A.; Navarrete-Magaña, M.; Gómez, R. N Doped-TiO2 Coupled to BiVO4 with High Performance in Photodegradation of Ofloxacin Antibiotic and Rhodamine B Dye under Visible Light. Catal. Today 2021, 394, 445–457.
70. Sharma, S.; Kumar, N.; Mari, B.; Chauhan, N.S.; Mittal, A.; Maken, S.; Kumari, K. Solution Combustion Synthesized TiO2/Bi2O3/CuO Nano-Composites and Their Photocatalytic Activity Using Visible LEDs Assisted Photoreactor. Inorg. Chem. Commun. 2021, 125, 108418.
71. Chawla, H.; Chandra, A.; Ingole, P.P.; Garg, S. Recent Advancements in Enhancement of Photocatalytic Activity Using Bismuth-Based Metal Oxides Bi2MO6 (M = W, Mo, Cr) for Environmental Remediation and Clean Energy Production. J. Ind. Eng. Chem. 2021, 95, 1–15.
72. Li, H.; Zhang, Y.; Zhang, Q.; Wang, Y.; Fan, Y.; Gao, X.; Niu, J. Boosting Visible-Light Photocatalytic Degradation of Indomethacin by an Efficient and Photostable Ag3PO4/NG/WO3 Composites. Appl. Surf. Sci. 2019, 490, 481–491.
73. Iqbal, S.; Bahadur, A.; Javed, M.; Hakami, O.; Irfan, R.M.; Ahmad, Z.; AlObaid, A.; Al-Anazy, M.M.; Baghdadi, H.B.; Abd-Rabboh, H.S.M.; et al. Design Ag-Doped ZnO Heterostructure Photocatalyst with Sulfurized Graphitic C3N4 Showing Enhanced Photocatalytic Activity. Mater. Sci. Eng. B Solid-State Mater. Adv. Technol. 2021, 272, 115320.
74. Zhang, C.; Zhang, M.; Li, Y.; Shuai, D. Visible-Light-Driven Photocatalytic Disinfection of Human Adenovirus by a Novel Heterostructure of Oxygen-Doped Graphitic Carbon Nitride and Hydrothermal Carbonation Carbon. Appl. Catal. B Environ. 2019, 248, 11–21.